

## Physics and Modelling of a Negative Ion Source Prototype for the ITER Neutral Beam Injection

J.P. Boeuf<sup>a</sup>, G. Fubiani<sup>a</sup>, G. Hagelaar<sup>a</sup>, N. Kohen<sup>a</sup>, L. Pitchford<sup>a</sup>, P. Sarrailh<sup>a</sup>, and A. Simonin<sup>b</sup>

<sup>a</sup> LAPLACE, CNRS, Université Paul Sabatier, 118 Route de Narbonne, 31062 Toulouse, France

<sup>b</sup> CEA, DSM/IRFM/SCCP, CEA Cadarache F-13108 Saint-Paul-lez-Durance

ITER Organization, Route de Vinon sur Verdon, 13115 Saint Paul Lez Durance, France

*E-mail address:* [jpb@laplace.univ-tlse.fr](mailto:jpb@laplace.univ-tlse.fr)

**Abstract.** The injection of energetic neutral deuterium atoms will be one of the major heating methods of the ITER plasma. The neutral atom beam will be obtained by acceleration and collisional neutralization of negative ions extracted from an inductively coupled low pressure plasma source. This paper describes the first steps toward a fully self-consistent model of this negative ion source. The negative ion source is a “cold plasma” (electron temperature on the order of 10 eV) composed of a driver where power is inductively coupled to the plasma electrons, an expansion chamber including a magnetic filter, and the extraction grids. In this paper we present the first results of a 2D fluid model of the driver, expansion chamber and magnetic filter for an H<sub>2</sub> plasma, in conditions close to the ITER negative ion source. The results show a decrease of the gas density when the plasma is turned on, due to gas heating and to the neutral gas depletion induced by ionization. The low gas density leads to high electron temperature in the driver, and to saturation of the plasma density growth with power for pressure below 0.3-0.4 Pa. The H<sub>2</sub> temperature is in the 0.1 eV range while the H temperature is much larger (up to 1 eV) because hydrogen atoms are generated at high energies by dissociation of H<sub>2</sub> or ion recombination at the wall surface. The simulation results are globally consistent with recent experiments on the negative ion source developed at IPP Garching. Because of the large Hall parameter in the magnetic filter, electron transport across the filter is complex and the ability of a 2D fluid model to grasp this complexity is discussed.

### 1. Introduction

The ITER heating system will include two neutral beam injectors, each delivering a 16.5 MW beam of 1 MeV Deuterium atoms. In each injector, ions will be first created in a plasma source, then accelerated by a set of electrostatic grids and finally neutralized by colliding with neutral molecules. Because the collisional neutralization of D<sup>+</sup> ions is very inefficient at these energies, D<sup>-</sup> ions will be used instead. These injectors will have to deliver beams during up to 3600 s, and will have to require as low as possible maintenance. The RF inductively coupled plasma source (ICP) which is currently being developed at the Max-Planck-Institut für Plasmaphysik, Garching has been chosen as the reference design for negative ion source for the ITER neutral beam injectors.

The studied negative ion source prototype is composed of a driver, an expansion chamber and magnetic filter, and the negative ion extraction region. It is now generally agreed that negative ion production in the volume by dissociative attachment is not sufficient for the ITER requirements. In the sources developed at IPP Garching, negative ions are produced by impact of H atoms on the caesium coated plasma grid [1]. The negative ions produced on the grid surface next to the grid holes can be efficiently extracted before they are collisionally detached. This paper describes the first steps toward a complete model of the Negative Ion Source for the ITER neutral beam system, including driver, diffusion chamber, magnetic filter and extraction. The goal is to obtain a better qualitative insight in the physics of the source, to get a quantitative prediction of its main characteristics, to contribute to its optimization, and to help in the interpretation of the experimental results. One of the important outputs of the

model is the flux and energy of H atoms on the grid since most of the extracted negative ions are generated by H atom impact on the grid.

The paper is organized as follows. The assumptions of the negative ion source model are briefly discussed in section 2. The plasma properties deduced from the simulations without magnetic filter are discussed in section 3. Some comments on the magnetic filter and power coupling are given in sections 4 and 5 respectively.

## 2. Model the negative ion source

A 2D fluid model of the source has been developed. The equations which are used are given and discussed in details in a recent paper [2]. The model can be used in a cylindrical or rectangular geometry and is based on the following assumptions:

- Fluid description of electrons: continuity, momentum transport (drift-diffusion) and energy equation (assuming Maxwellian distribution) including magnetic field barrier.
- Fluid description of positive ions: continuity and momentum equation (including inertia terms); in the source conditions, the pressure term is negligible with respect to the electric force term. Negative ions are described by a drift-diffusion equation.
- The model does not assume quasi-neutrality and Poisson's equation is solved implicitly.
- For the results presented in sections 1. to 4, we limited ourselves to a simple case where we assumed that the power emitted by the antenna  $P_{tot}$  is totally absorbed by the electrons in the driver and that each electron absorbs the same amount of power. In that case, the source term for the electron energy equation  $P_{vol}$  is given by  $P_{vol} = P_{tot} \cdot n_e / N_e$ , where  $N_e$  is the total number of electrons in the driver and  $n_e$  is the electron number density. However, the RF field (1 MHz) induced by the coil current and its coupling with the electrons can also be described in details by the code, and this part of the model is presented in section 5.
- Neutral transport can be described by Navier-Stokes equations or using a more accurate Direct Simulation Monte Carlo (DSMC). The Navier-Stokes module is used in the results presented here.
- A complete set of kinetic reactions for hydrogen has been implemented. The hydrogen vibrational population is not calculated self-consistently at the moment and electron attachment in the source volume is therefore not self-consistent (the fractional concentration of the vibrationally excited states is fixed, and a global electron attachment cross-section is used). The production of negative ions at the grid surface is not included in these preliminary simulations.

The fluid model describes self-consistently the neutral and plasma transport and reactions, including the magnetic field barrier. In order to better understand and describe transport across the magnetic field barrier, explicit as well as implicit Particle-In-Cell (PIC) simulations are also being developed.

The model has been applied to an ITER-like negative ion source similar to one of the prototypes developed at IPP Garching [3]. The source is composed of a driver where the plasma is generated by RF (1 MHz) inductive coupling. The driver is followed by an expansion chamber. At the end of the expansion chamber and in front of the extraction grids,

a magnetic field filter is used to limit the flux and energy of electrons flowing to the extraction region.

The geometry of the source simulated in the model is shown in FIG. 1. In the ITER negative ion source prototypes, the driver is a cylinder and the expansion chamber is a rectangular box; the magnetic field is parallel to the width of the rectangular expansion chamber. Since the model is two-dimensional it was necessary to use a rectangular (and not cylindrical) geometry to represent properly the magnetic filter region. The dimensions of the simulated rectangular source shown in FIG. 1 are deduced from the dimensions of the real prototypes by simple and approximate scaling laws [4].

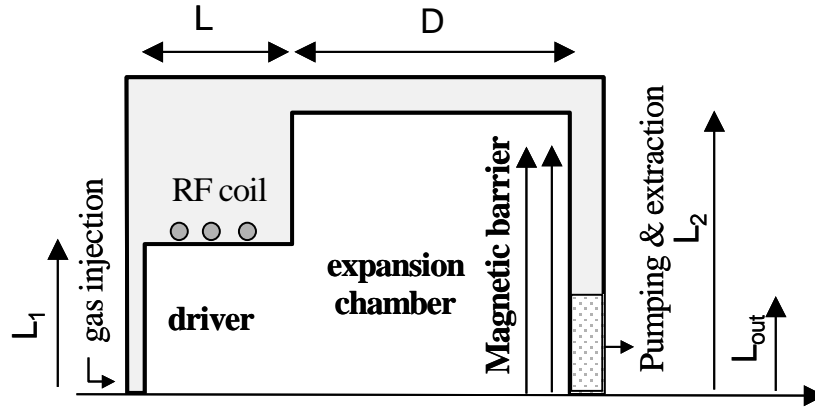


FIG. 1: Rectangular source geometry used in the model. The dimensions are:  $L_1=8$  cm,  $L=9$  cm,  $D=16$  cm, and  $L_2=16$  cm, with  $L_{out}=6$  cm.

### 3. Plasma Properties without magnetic filter

Calculations have been performed under conditions of pressure and power similar to those of the negative ion source prototype experimentally studied by McNeely et al. [2]. The total power absorbed by the plasma was an input of the simulation (constant power absorbed per electron in the driver). The operating pressure was fixed in the simulations before the plasma was turned on, by adjusting the hydrogen mass flow rate and running the Navier Stokes model. FIG. 2 and FIG. 3 show typical results for the distributions of plasma density, potential, and neutral concentration and temperature. The calculated plasma density is on the order of  $0.5 \cdot 10^{18} \text{ m}^{-3}$  i.e. about 5 times less than the density measured by McNeely et al. [3]. The calculated plasma density is strongly dependant on the gas density (i.e. on the operating pressure).

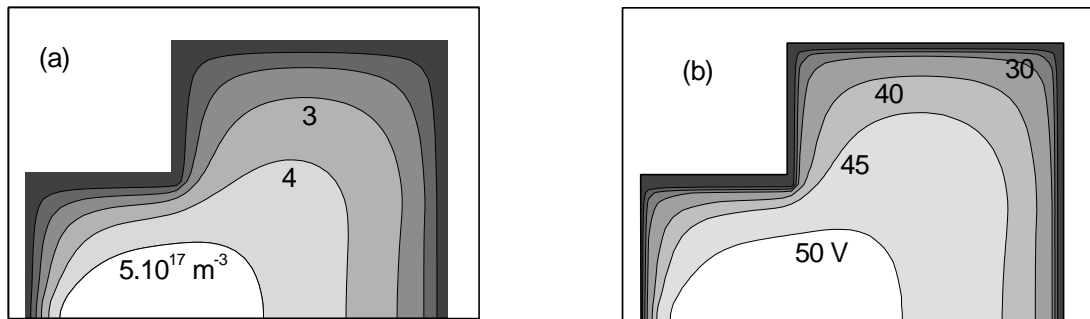


FIG. 2: Space distributions of (a) plasma density, (b) plasma potential for an input power of 60 kW at 0.3 Pa, without magnetic field. The calculated electron temperature is quasi-uniform, around 13 eV. Darker grey corresponds to smaller values.

The discrepancy between experimental measurements and calculations could be due to uncertainties in the gas pressure and density. Another possible source of discrepancy is the effect of the ponderomotive force. At the low frequency (1 MHz) and high power of the RF source, the ponderomotive force [1] (which is not included in the results presented here) can compress the plasma and increase the plasma density.

The calculated concentrations and temperatures of hydrogen molecules and atoms are shown in FIG. 3.

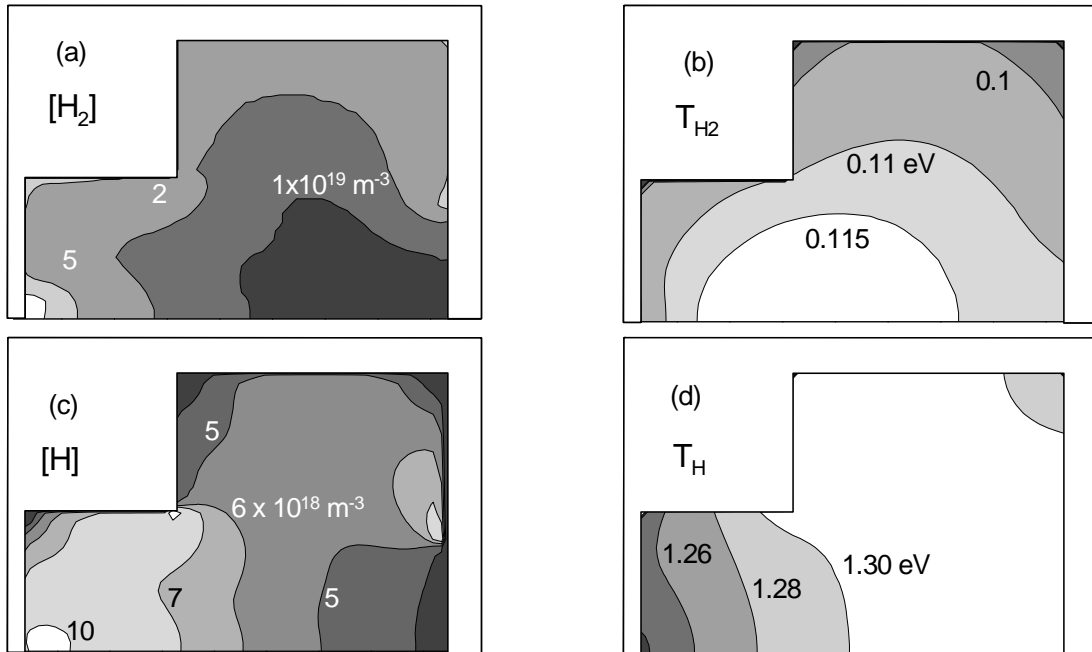


FIG. 3: Space distributions of (a),  $H_2$  density, (b),  $H_2$  temperature, (c),  $H$  density, and, (d),  $H$  temperature, in the conditions of Fig. 2 (60 kW, 0.3 Pa, rectangular geometry).

The molecular hydrogen concentration is on the order of  $10^{19} \text{ m}^{-3}$  in the extraction region. This is much smaller than the density corresponding to a pressure of 0.3 Pa at ambient temperature ( $7 \cdot 10^{19} \text{ m}^{-3}$ ). This low density is due to the increase in gas temperature when the plasma is turned on, and to neutral depletion due to ionization. The density of atomic hydrogen also shown in FIG. 3 is about 60 % of the density of molecular hydrogen in the extraction region. The temperatures of molecular and atomic hydrogen are very different, as shown in FIGs. 3b and 3d respectively. The  $H_2$  temperature is on the order of 0.1 eV while the  $H$  temperature reaches values on the order of 1 eV or more. The relative high temperature of  $H$  atoms is due to 1),  $H$  atoms generation with an energy around 3 eV during electron impact dissociation, and 2), recombination of energetic  $H^+$  at the walls.

The distribution of the different species concentration (electron,  $H^+$ ,  $H_2^+$ ,  $H_3^+$ ,  $H$ , and  $H_2$ ) along the discharge axis are shown on FIG. 4. We see that  $H_2^+$  is the dominant ion in the driver while the density of  $H^+$  becomes larger in the expansion chamber.

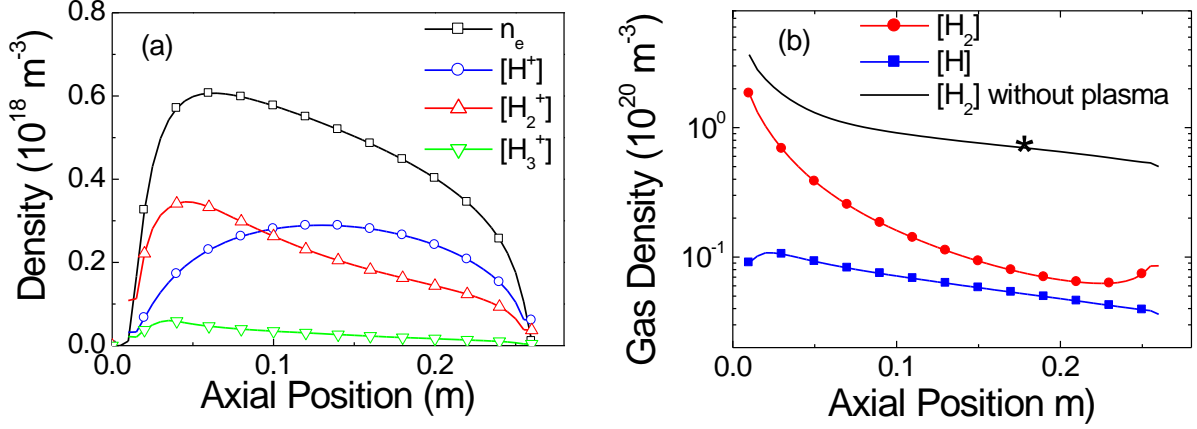


FIG. 4: Distribution, along the discharge axis of (a) charged particles densities, and (b) neutral densities, in the conditions of Fig.2 (60 kW, 0.3 Pa). The gas density without plasma is also shown for comparison in Fig. 4b. The star symbol indicates the location where the pressure is exactly equal to 0.3 Pa (gas density  $7 \cdot 10^{19} \text{ m}^{-3}$  at 300 K) in the chamber, before the plasma is turned on.

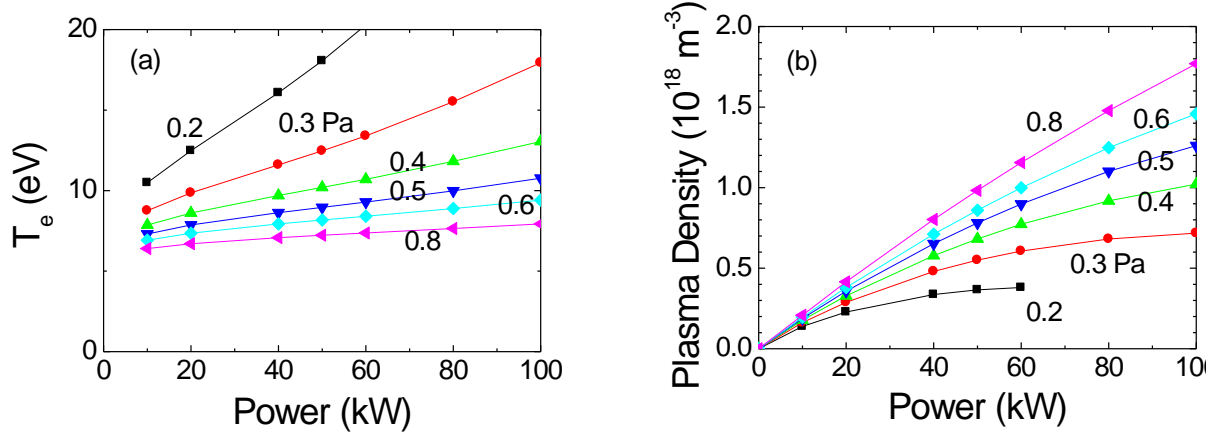


FIG. 5: (a) Electron temperature, and, (b), maximum electron density (the maximum density is in the driver) as a function of input power, for different gas pressures

The variations of electron temperature and density as a function of absorbed power for different pressure are shown in FIG. 5.

We see on FIG. 5 that the electron temperature is almost insensitive to the value of the absorbed power at high enough pressure and increases sharply with power at pressure on the order of below 0.3-0.4 Pa. On the other hand, the plasma density for a given power increases with increasing pressure. The plasma density at constant pressure increases with power, as expected, but tends to saturate at pressure below 0.3 Pa. The electron temperature and density and the trends of their variations with power and pressure are in reasonable agreement with the Langmuir probe [3] and spectroscopic [5] measurements of the IPP Garching group.

The variations of plasma temperature and electron density with power and pressure can be understood on the basis of very simple scaling laws obtained by writing global particle and power balance equations in the source. The simplest form of a global particle balance equation when charged particle production is due to direct ionization and charged particle losses are due to recombination at the walls can be obtained by writing that the volume integrated ionization rate is equal to the wall surface integrated charged particle losses:

$$nn_g k_i V = \alpha n u_B S$$

where  $n$  is the plasma density,  $n_g$  is the gas density,  $k_i$  is the ionization rate (assumed to be constant in space, which is a good approximation here),  $V$  the discharge volume,  $u_B$  the Bohm velocity,  $S$  the wall surface, and  $\alpha$  a coefficient accounting for the fact that the plasma density is smaller at the sheath edge than in the bulk plasma.  $k_i$  and  $u_B$  are function of the electron temperature. Therefore,

$$\frac{k_i(T_e)}{u_B T_e} = \frac{1}{n_g d_{eff}}$$

This equation shows that the electron temperature only depends on the gas density, and on an effective plasma dimension,  $d_{eff} = \alpha V/S$  proportional to the source volume/wall surface ratio. One can therefore understand that, for a given input power, the electron temperature must be larger at 0.3 Pa than, e.g. at 0.8 Pa. The equation above also shows that, if the gas density is fixed, the electron temperature should be practically independent of power. In our conditions the gas density is not fixed because of the increase in gas temperature with power and because of the gas depletion due to ionization and gas heating. The gas density decreases with increasing power, therefore volume ionization decreases and a larger electron temperature is needed to balance the losses to the walls. The ionization rate  $k_i$  in hydrogen, like in other gases, increases with electron temperature and tends to reach a limit and eventually decay at high electron temperatures.

From a simple power equation one could also show that the plasma density should increase linearly with absorbed power at constant electron temperature. But since the electron temperature increases with power because of the neutral density decrease (see above), the increase of plasma density with power is less than linear and tends to saturate as seen in FIG. 5b.

Since the extracted negative ions are mainly produced by the impact of hydrogen atoms on the grid surface, an important output from the model is the atomic hydrogen flux to the grid. The calculated H and H<sup>+</sup> fluxes and energy fluxes to the grid are shown as a function of power on FIG. 6 for a pressure of 0.3 Pa. The calculated maximum H flux to the grid ( $10^{22} \text{ m}^{-2} \cdot \text{s}^{-1}$ ) corresponds to an equivalent current density of H atoms on the grid of about  $1600 \text{ A} \cdot \text{m}^{-2}$ . Assuming a yield of about 0.2 H<sup>-</sup> emitted by the grid surface per H incoming atom (this is consistent with values found in the literature, e.g. Ref. [6]), this would lead to a negative ion density of about  $320 \text{ A} \cdot \text{m}^{-2}$ .

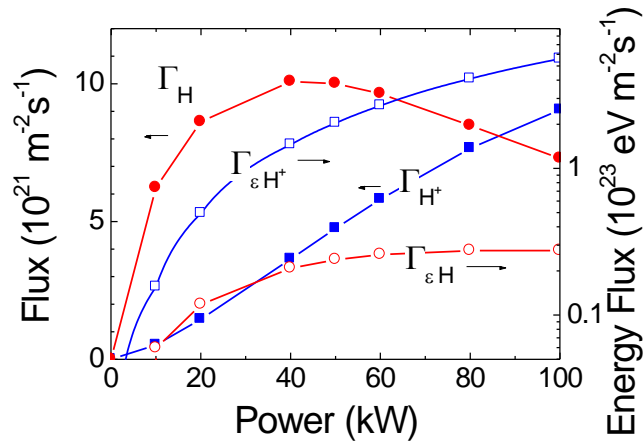


FIG. 6: Averaged H flux ( $\Gamma_H$ , full circle symbols), and H<sup>+</sup> flux ( $\Gamma_{H^+}$ , open circle symbols) on the plasma grid, and averaged H energy flux ( $\Gamma_{\epsilon H}$ , full circle symbols), and H<sup>+</sup> energy flux ( $\Gamma_{\epsilon H^+}$ , open circle symbols) on the plasma grid, as a function of input power at 0.3 Pa.

$300 \text{ A}\cdot\text{m}^{-2}$  is the order of magnitude required for the ITER source, but since one can expect that only a fraction of the negative ions produced on the surface can be extracted (20% according to Ref. [7]), it seems that the calculated H flux is actually too small. Positive ions impacting the grid could also contribute to the production of negative ions on the surface but this question needs clarification.

#### **4. Plasma Transport Across the Magnetic Filter**

Calculations have been performed including a magnetic filter, with a magnetic field in the simulation domain, parallel to the extracting grid, assuming classical, collisional transport across the B field. The results show strong plasma oscillations when a magnetic field similar to the experimental one is used. These oscillations are due to the low neutral density and large Hall parameter (ratio of electron angular cyclotron frequency and electron-neutral collision frequency) in the filter region. The oscillations are damped if a smaller magnetic field is used and if electron transport across the magnetic field is artificially increased. In that case, as expected, a decrease of the electron flux and electron temperature across the magnetic filter is observed. The decrease of the electron temperature in the filter region is associated with an increase of the electron temperature outside the filter.

The model must be improved to describe more realistically the magnetic filter region. Work is continuing in a 2D geometry where the magnetic field is taken perpendicular to the simulation domain. Because of the low gas density in the extraction region it is also possible that instabilities develop to increase electron transport across the magnetic field barrier. Since it is not clear whether such instabilities can be described with a fluid approach, explicit and implicit Particle-In-Cell simulations are also developed to better understand electron transport across the filter.

#### **5. Energy Coupling in the Driver**

The results presented in this paper have been obtained assuming that the power absorbed per electron is uniformly distributed in the driver. A more detailed model describing the energy coupling (Maxwell equations plus electron equations) has also been developed and is described in Ref. [2]. Nonlocal electron kinetics, leading to the formation of an “anomalous skin” and collisionless electron heating, is included in the model through an effective electron viscosity. This gives results that are consistent with experiments under relatively low power conditions (such as those used in ICP sources for surface treatment). Under the low-frequency, high-power conditions of the Garching source the RF magnetic field force must be included. This force tends to push the plasma away from the walls (from the RF coils) in the driver (ponderomotive force) and can also change the anomalous skin effect. These effects strongly increase with decreasing RF frequency. The ponderomotive effect has been included in the model. Preliminary results show an increase of plasma density in the driver due to plasma compression by the ponderomotive force at RF frequencies above 5 MHz, but the model fails to provide steady-state solutions at the operating frequency of 1 MHz of the IPP sources, because the ponderomotive force becomes so excessively strong that it expulses the plasma from the driver, which is clearly not realistic. Work is continuing to solve this problem.

#### **6. Summary and conclusion**

Important progress has been made in the model development of the negative ion source under conditions close to those of the ITER prototypes developed and studied at IPP Garching. The model can now be used to help understanding the physics and the scaling parameters.

Comparisons with experiments show that the model reproduces well the trends of variations of the main parameters with power and pressure. Work must be continued to perform more detailed quantitative comparisons and to understand the reasons for discrepancies. A better description of electron transport through the magnetic filter is however still needed to be able to characterize self-consistently the plasma in the extraction region. A proper quantification of the ponderomotive effects in the driver in the operating conditions of the IPP sources is still needed. Work is continuing along these lines.

### **Acknowledgements**

This work has been performed in the frame of the ITER-NIS project of the French National Research Agency (ANR, BLAN08-2\_310122). Support from EFDA, CEA and from the French Fédération de Recherche sur la Fusion Magnétique is also acknowledged. The authors would like to thank U. Fantz, P. Franzen, P. McNeely, and colleagues from the IPP group in Garching for stimulating discussions.

### **References**

- [1] E. Speth et al. Nucl. Fusion **46** S220 (2006)
- [2] G.J.M. Hagelaar, G. Fubiani, J.P. Boeuf, “Self-consistent model of an inductively coupled negative ion source for neutral beam injection – I General model description”, to appear in Plasma Sources, Sci. Technol.
- [3] P. McNeely, S. V. Dudin, S. Christ-Koch, U. Fantz and the NNBI Team, Plasma Sources Sci. Technol. **18** 014011 (2009)
- [4] J.P. Boeuf, G.J.M. Hagelaar, P. Sarrailh, G. Fubiani, N. Kohen , “Self-consistent model of an inductively coupled negative ion source for neutral beam injection - II Application to an ITER-type source, to appear in Plasma Sources, Sci. Technol.
- [5] U. Fantz, H. Falter, P. Franzen, D. Wunderlich, M. Berger, A. Lorenz, W. Kraus, P. McNeely, R. Riedl and E. Speth, Nucl. Fusion **46** S297–S306 (2006)
- [6] McAdams and E. Surrey, in Negative Ions, Beams and Sources: 1<sup>st</sup> International Symposium, edited by E. Surrey and A. Simonin, American Institute of Physics Conference Proceedings 1097 p. 89 (2009)
- [7] R. Gutser, D. Wunderlich, U. Fantz, and the NNBI-Team, Plasma Phys. Control. Fusion **51** 045005 (2009)